Journal of Immunological Methods 473 (2019) 112644

Contents lists available at ScienceDirect

Journal of Immunological Methods

journal homepage: www.elsevier.com/locate/jim

Research paper

Monitoring kinetics reveals critical parameters of IgA-dependent granulocyte-mediated anti-tumor cell cytotoxicity

Anabel Zwick[a], Muriel Bernhard[a], Arne Knoerck[b], Maximilian Linxweiler[c], Bernhard Schick[c], Joana Heinzelmann[d], Sigrun Smola[a], Stefan Lohse[a,*]

[a] Institute of Virology, Saarland University Medical Center, 66421 Homburg, Germany
[b] Department of Biophysics, Center of Integrative Physiology and Molecular Medicine (CIPMM), Saarland University, 66421 Homburg, Germany
[c] Department of Otorhinolaryngology, Head and Neck Surgery, Saarland University Medical Center, 66421 Homburg, Saar, Germany
[d] Department of Urology, Saarland University Medical Center, 66421 Homburg, Saar, Germany

ARTICLE INFO

Keywords:
Immunotherapy
Granulocyte cytotoxicity assay
EGFR
IgA
Impedance
HNSCC

ABSTRACT

Human IgA antibodies effectively engage myeloid cells for the FcαRI-dependent antibody-dependent cell-mediated cytotoxicity (ADCC) of tumor cells. Established methods to investigate ADCC are the ^{51}chromium and Calcein release assays. Their critical limitations are the end-point measurement, the unspecific release of the probes, the requirement of target cells in suspension and thus do not reflect physiologic conditions of adherently growing cells. Here we report the label-free real-time monitoring of granulocyte-mediated ADCC using an impedance-based method. We investigated the efficacy of an engineered epidermal growth factor receptor (EGFR)-directed IgA2 antibody to engage neutrophils for ADCC against a panel of adherently growing EGFR-expressing cancer cell lines majorly head and neck squamous cell carcinoma (HNSCC). The impedance assay allowed the documentation of the IgA-neutrophil-and FcαRI-signaling dependent ADCC of adherently growing target cells. While at a short-term it provided comparable results to release assays, in the long run real time monitoring also revealed cell-line specific kinetics and long-term efficacy. Although short-term results may depend on EGFR expression, long-term efficacy did not correlate with the surface level of EGFR nor of the myeloid checkpoint CD47 pointing to additional critical parameters to predict the treatment efficacy. Real-time monitoring of neutrophil-mediated ADCC allowed documenting effector cell activity and exhaustion. Along with excess expression of Mac-1 ligands, which may explain the target cell resistance, this eventually leads to tumor cell outgrowth at later time points. In conclusion, the impedance assay provides valuable information on the kinetics, effector cell performance, efficacy and critical parameters of IgA-dependent granulocyte-mediated cytotoxicity and is expected to become an important tool in its evaluation.

1. Introduction

The epidermal growth factor receptor (EGFR) is frequently overexpressed and critically involved in the carcinogenesis of head and neck cancer (HNSCC) (Hanahan and Weinberg, 2011; Hynes and MacDonald, 2009; Grandis and Tweardy, 1993; Szabó et al., 2011; Leemans et al., 2011). In addition, HNSCC is further characterized by the infiltration of myeloid cells such as neutrophils (Dumitru et al., 2013; Galdiero et al., 2013). Several studies report that the local micromilieu provides respective chemokines and stimuli suppressing apoptosis and inducing a tumor-promoting polarization of granulocytes (Trellakis et al., 2011; Dumitru et al., 2013; Galdiero et al., 2013; Valero et al., 2016). Patients with HNSCC and high levels of circulating as well as infiltrating neutrophils are indeed at higher risk of poor prognosis. There is a mounting evidence that myeloid cells are critically involved in the manifestation, progression and invasion of cancer and display a promising effector cell population for immunotherapy (Braster et al., 2014; Uribe-Querol and Rosales, 2015; Treffers et al., 2016; Smola, 2017). In particular,

Abbreviations: ADCC, antibody-dependent cell-mediated cytotoxicity; AUC, area under curve; CFSE, Carboxyfluorescein succinimidyl ester; CRA, ^{51}chromium release assay; CXCL4, CXCL8 C-X-C motif chemokine ligand 4, 8; EGFR, epidermal growth factor receptor; FcαRI, Fc-alpha receptor I; G-CSF, granulocyte colony stimulating factor; GM-CSF, granulocyte macrophage colony stimulating factor; HNSCC, head and neck squamous cell carcinoma; ICAM, intercellular adhesion molecule; IgA, IgG immunoglobulin A, G; LTB_4, leukotriene B_4; MTT, 3-[4,5 Dimethylthiazol-2-yl]-2,5-diphenyltetrazolium-bromid; nCI, normalized Cell Index; NET, neutrophil extracellular trap; NK, cells natural killer cells; PVDF, polyvinylidene difluoride membranes; ROS, reactive oxygen species

* Corresponding author at: Institute of Virology, Saarland University Medical Center, Kirrberger Str. Building 47, 66421 Homburg, Germany.
E-mail address: stefan.lohse@uni-saarland.de (S. Lohse).

https://doi.org/10.1016/j.jim.2019.112644
Received 17 January 2019; Received in revised form 26 June 2019; Accepted 8 August 2019
Available online 09 August 2019

neutrophils were recently described as promising effector cells in antibody-based therapy of cancer (Heemskerk and van Egmond, 2018). Hence, immunotherapeutic approaches effectively engaging neutrophils for ADCC could display an interesting therapeutic perspective for the treatment of HNSCC.

Notably, human IgA antibodies engage granulocytes for tumor cell killing more effectively than comparable IgG1 antibodies (Brandsma et al., 2015; Lohse et al., 2016) and were recently engineered for an enhanced in vivo FcαRI-dependent myeloid cell-mediated anti-tumor cell activity (Lohse et al., 2016). Myeloid cell engagement for ADCC by human IgA antibodies has been reported for different tumor antigens and entities in vitro and in animal trials (Boross et al., 2013; Brandsma et al., 2015; Heineke and van Egmond, 2016; Lohse et al., 2016, 2018). FcαRI is the responsible Fc receptor and expressed on myeloid cells, such as granulocyte, monocytes and macrophages (Woof and Russell, 2011; Heemskerk and van Egmond, 2018). Myeloid cells are activated for the important Fc-mediated effector mechanism ADCC using EGFR-specific IgA antibodies (Lohse et al., 2016).

Established methods to investigate ADCC are release assays using the radioactive ^{51}chromium, its fluorescent alternative Calcein or more recently with Carboxyfluorescein succinimidyl ester (CFSE) (Brunner et al., 1968; Wierda et al., 1989; Roden et al., 1999; Yamashita et al., 2016). Technically, cells are labeled with the respective probe, which is released upon cell lysis and measured using a gamma-, scintillation-, fluorescence-counter, or by flow cytometry, respectively. These methods have various disadvantages: 1) They are end-point assays, 2) they use target cells in suspension and 3) there is a significant time-dependent spontaneous release (Peper et al., 2014). 4) Many target cells do not take up the probes or release them spontaneously without being killed, which limits the choice of targets (Peper et al., 2014). 5) The hazardous radioactive isotype requires an appropriate infrastructure, training, regulatory admittance and is cost intensive due to the short half-life and waste disposal. 6) These methods do not allow an appropriate documentation of kinetics and long-term observations of IgA-granulocyte-mediated ADCC of adherently growing target cells.

The impedance-based technology allows the label-free real-time evaluation of cytotoxic effects against adherently growing cells (Peper et al., 2014; Oberg et al., 2014). Particularly for solid cancer cells adherence displays a more physiologic condition than the suspension conditions of both ^{51}chromium (CRA) and Calcein release assays (Peper et al., 2014; Oberg et al., 2014). In impedance-based assays, the target cells grow adherently on gold electrodes on the plate's bottom. This results in increased impedance to an electric current, which in turn is reduced upon cell killing related detachment or disintegration. This method permits the real-time monitoring of cell-mediated cytotoxicity or ADCC providing reproducible results for NK- and T-cell-mediated killing for instance (Glamann and Hansen, 2006; Yamashita-Kashima et al., 2011; Kute et al., 2012; Seidel et al., 2014; Peper et al., 2014).

In this report, we used this impedance-based technology to investigate the capacity of the engineered EGFR-directed 225-IgA2.0 antibody to mediate FcαRI- and granulocyte-mediated cytotoxicity against a panel of adherently growing EGFR-expressing tumor cells. This is the first report that provides insights into the underlying kinetics, long-time effectivity, effector cell performance and on critical parameters of the IgA-dependent granulocyte-mediated ADCC.

2. Material and methods

2.1. Ethical statement

The local Ethics Committee of the Saarland (Ärztekammer des Saarlandes, Saarbrücken, Germany) in accordance with the Declaration of Helsinki approved experiments with human material used in this study.

2.2. Cell lines

The human head and neck squamous cell carcinoma cell lines CAL-33 (tongue), FaDu (hypopharynx), HN (oral), HSC-4 (aero-digestive tract), SAS (tongue), SAT (upper aero-digestive tract), UM-SCC-1 (floor of the mouth) were maintained in DMEM supplemented with 10% FBS, 100 U/mL penicillin, and 100 µg/mL streptomycin. Cell lines were kindly provided in 2016 by Dr. Malte Kriegs (CAL-33, SAS, SAT, HSC-4; University Medical Center Hamburg-Eppendorf, Oncology Center, Department for Radiotherapy and Radio-Oncology) and Dr. Maximilian Linxweiler (HN, UM-SCC-1, FaDu; Department of Otorhinolaryngology, Head and Neck Surgery; Saarland University Medical Centre, Homburg, Germany). The human epidermoid carcinoma cell line A-431 (DSMZ, ACC-91, obtained 2015, authenticated in 2018 by Multiplexion, Heidelberg, Germany) was used as reference line (Lohse et al., 2016) and cultured in RPMI 1640 containing 10% heat-inactivated FBS, 100 U/mL penicillin, and 100 µg/mL streptomycin. The human esophageal squamous carcinoma cell line KYSE-30 (German Collection of Microorganisms and Cell Cultures (DSMZ), Braunschweig, Germany, ACC-351, obtained 2015) was kept in 45% RPMI 1640 with 45% Ham's F12, 10% FBS, and 1% antibiotics (100 U/mL penicillin, 100 µg/mL streptomycin, all media and additives from Sigma-Aldrich, Schnelldorf, Germany). We conducted mycoplasma specific PCRs on a regular basis of once per month.

2.3. Antibodies

Monomeric engineered 225-IgA2m(1)-N166G-P221R-C331S-N337T-I338L-T339S-dC471-dY472 further named 225-IgA2.0 (abbreviated as IgA2.0 in figures) was produced using the variable regions of the m225 antibody and the engineered IgA2m(1) constant region as previously described (Lohse et al., 2016). Antibody was produced in the lab of Prof. Dr. Thomas Valerius (University Hospital Schleswig-Holstein, Division of Stem Cell Transplantation and Immunotherapy, II. Department of Internal Medicine). ChromPure human Serum IgA purchased from Jackson served as IgA isotype control. FcαRI was blocked with 10 µg/ml anti-human CD89 antibody A59 (BioLegend, San Diego, USA; 354102).

2.4. Isolation of human effector cells

Mononuclear cells were separated from citrate anticoagulated blood drawn from healthy volunteers (written informed consent was obtained) by Ficoll (FicoLiteH 1.077 g/ml, Linaris, Wertheim-Bettingen, Germany) gradient centrifugation. Red blood cells were removed from the bottom layer, containing the granulocytes, by cold hypotonic lysis. Purity of granulocytes was > 95% as assessed by flow cytometry using a mouse anti human CD66b directed antibody (5 µl/test, Biolegend, San Diego, USA; 305102) and an AlexaFluor-488 (AF488) goat anti-mouse IgG (Fisher Scientific, Schwerte, Germany, A11029). Contaminations with monocytes were excluded by staining with an anti-human CD14-APC labeled (555399, isotype control 555576, both BD Biosciences) (Suppl. Fig. 1).

2.5. Impedance assay

The impedance-based x-CELLigence system (ACEA Bioscience Inc., San Diego, CA, USA) was placed at 37 °C in a humidified 5% CO_2 incubator. 2×10^4 cells per well were seeded in 96-well micro E-plate (#2801035, glass bottom, ACEA Bioscience) and monitored 24 h every 15 min. At the maximum Cell Index (confluence) after 24 h antibodies and immune cells were added as indicated. Medium with 1% Triton X-100 was used as cytolysis control. Cells were monitored every minute for 4 h and thereafter every 15 min for at least 24 h. For secondary treatment, the measurement was paused 6 h after first treatment and fresh granulocytes of the same donor with or without fresh antibody

were added. Wortmannin (SelleckChem, Houston, TX USA) was supplemented together with antibodies and granulocytes or granulocytes were preincubated for 30 min, washed 3 times with RPMI to remove residual inhibitor and then added to the targets. Target cells were pretreated after growing for 24 h on E-plates with Chloroquine (SelleckChem) for 30 min, washed 3 times with RPMI to remove residual inhibitor before antibodies and immune cells were added.

2.6. Calcein assay

2×10^4 A-431 target cells/well were labeled for 30 min at 37 °C with 10 μM Calcein-AM (Fisher Scientific, C3099) either in suspension or grown to confluence for 24 h in 96-well-plates. After three consecutive washing steps isolated effector cells were added with an effector to target cell ratio (E:T ratio) of 40:1. Antibodies were added to the microtiter plates in triplicates as indicated. For maximum release labeled target cells were treated with 1% Triton X-100 (Sigma-Aldrich, Schnelldorf, Germany) or left untreated for basal release. After 4 h incubation at 37 °C, plates were centrifuged; supernatants were transferred into black 96-well plates with clear flat bottom (Sigma-Aldrich) and fluorescence measured in the Victor II plate reader (PerkinElmer, Waltham, MA, USA). Percentage of cellular cytotoxicity was calculated using the equation: % specific lysis = (experimental release − basal release)/(maximal release − basal release). Antibody-independent cytotoxicity (effectors without target antibodies) or effector-independent cytotoxicity (target antibodies without effectors) was not observed.

2.7. Flow cytometry

For EGFR (mouse anti-human EGFR-specific antibody, BD Biosciences, 555996), ICAM1 (mouse anti-human ICAM1-specific antibody, Fisher Scientific, MA1-19123) and CD47 (mouse anti-human CD47-specific antibody, BD Biosciences, 556044) surface analysis, cells were seeded and grown to 80% confluence, trypsinized and stained with 50 μg/ml antibody per 100.000 cells for 1 h on ice. After washing bound antibody was stained with m-IgGκ PE conjugated secondary binding protein (sc-516141, Santa Cruz, Dallas, TX, USA) and measured with a FACS Canto II 8 (BD Biosciences). Relative fluorescence intensity was calculated using the following equation: mean fluorescence intensity specific Ab/mean fluorescence intensity control Ab, relative MFI was calculated over all samples. For apoptosis assay, cells from ADCC assay were harvested at given time points and surface was labeled with BV421-labeled CD66b antibody (5 μl/test, BD Biosciences, 562940; Clone G10F5). After washing, cells were stained in Annexin buffer (10 mM Hepes, pH 7.4; 140 mM NaCl; 2,5 mM $CaCl_2$) containing APC-labeled Annexin V (5 μl/test, BD Biosciences, 550474) and propidium iodide (PI; 1 μg/ml Sigma-Aldrich P4864). A minimum of 1×10^4 cells were recorded and living granulocytes were analyzed with FACS Diva Software as $CD66b^+/Annexin\ V^-/PI^-$.

2.8. Immunofluorescence

A-431 target cells were harvested from E-plates after 72 h impedance-ADCC assay by trypsinization and reseeded onto black 96-well plates with μ-clear flat bottom (Sigma-Aldrich, M0562-32EA). After recovering and growing for 48 h cells were fixed with 4% paraformaldehyde (Sigma-Aldrich) and stained with CD47 (mouse anti-human CD47-specific antibody, BD Biosciences, 556044, 1:200) and an AlexaFluor488-labeled goat-anti-mouse-IgG (1:100, Thermo). Nuclear staining was performed using DAPI (Sigma-Aldrich). Pictures were recorded using a LeicaDMI6000 fluorescence microscope and LAS Suite 3.8 as software (both Leica, Wetzlar, Germany).

2.9. Live cell imaging

5×10^3 A-431 target cells/well were grown for 24 h in 96 well black microplates with clear flat bottom (Sigma-Aldrich). Prior to imaging GM-CSF stimulated granulocytes were added at an E:T ratio of 40:1 together with 225-IgA2.0 antibody or isotype control (c = 10 μg/ml). Images were acquired with ImageXpress Micro XLS Widefield High-Content Analysis System (Molecular Devices, San José, CA, USA) every 5 min for 5 h.

2.10. Enzyme-linked immunosorbent assay (ELISA)

Supernatants from ADCC assays of four different effector cell donors were collected and stored at −80 °C. LTB_4 were quantified using the LTB_4 Parameter Assay kit (R&D Systems, Wiesbaden, Germany, KGE006B) according to the manufacturer's instructions.

2.11. Quantitative RT-PCR

RNA was isolated from 10 cm dishes (Sigma-Aldrich) with cells were seeded and grown to 80% confluence. cDNA was generated from 1 μg RNA with SuperscriptII (Fisher Scientific). The Universal Probe System (Roche, Basel, Swiss) and the LightCycler 480II (Roche, Mannheim, Germany) were used to perform qRT-PCR. Expression levels of ICAM1 and ICAM2 were normalized to ribosomal protein L13A (RPL13A), which is a well-proven housekeeping gene in keratinocytes (Marthaler et al., 2017, primers and probes Suppl. Table 1). Intron-spanning oligonucleotides were designed with the Universal Probe Library (UPL) Assay Design Center version 2.53 (Roche).

2.12. Data processing and statistical analyses

Data were generated from at least three independent experiments with triplicates. Graphical, correlation and statistical analyses were performed using GraphPad Prism 7.02 (GraphPad Software, San Diego, USA). Group data are reported as mean ± SEM. Significance was determined by two-way Anova repeated measures test with Bonferroni's post hoc correction. Significance was accepted when p-values were ≤ 0.05.

3. Results

3.1. The Calcein release assay requires target cells in suspension

The CRA and Calcein release assays are conducted using target cells in suspension. These are labeled with the respective probe and cultured together with effector cells and antibodies. Similar to previous experiments using the CRA (Lohse et al., 2016), treatment of Calcein-labeled EGFR expressing A-431 target cells in suspension with granulocytes (E:T = 40:1) resulted in 36.3% (± 6.4%) specific lysis in the presence of 10 μg/ml 225-IgA2.0 antibody at 4 h after treatment (Fig. 1A). Addition of 25 nM GM-CSF increased the specific lysis up to 65.5% (± 6.2%). The target cell lysis was dependent on FcαRI-interaction since 10 μg/ml of the FcαRI-specific antibody A59 completely blocked the effect (Fig. 1A).

However, when Calcein-labeled A-431 cells were tested under the more physiologic condition of adherence, no significant Calcein release within 4 h was detected (Fig. 1B). Moreover, target cells treated with granulocytes and 225-IgA2.0 released even less Calcein than the untreated control. These results indicate that release assays apparently require target cells in suspension and are therefore not applicable to investigate ADCC of adherently growing solid cancer cells.

3.2. The impedance-based assay allows the real-time documentation of the IgA-dependent granulocyte-mediated ADCC using adherently growing target cells

Next, we analyzed if the impedance-based measurement of ADCC (Peper et al., 2014) is applicable to investigate the IgA-dependent

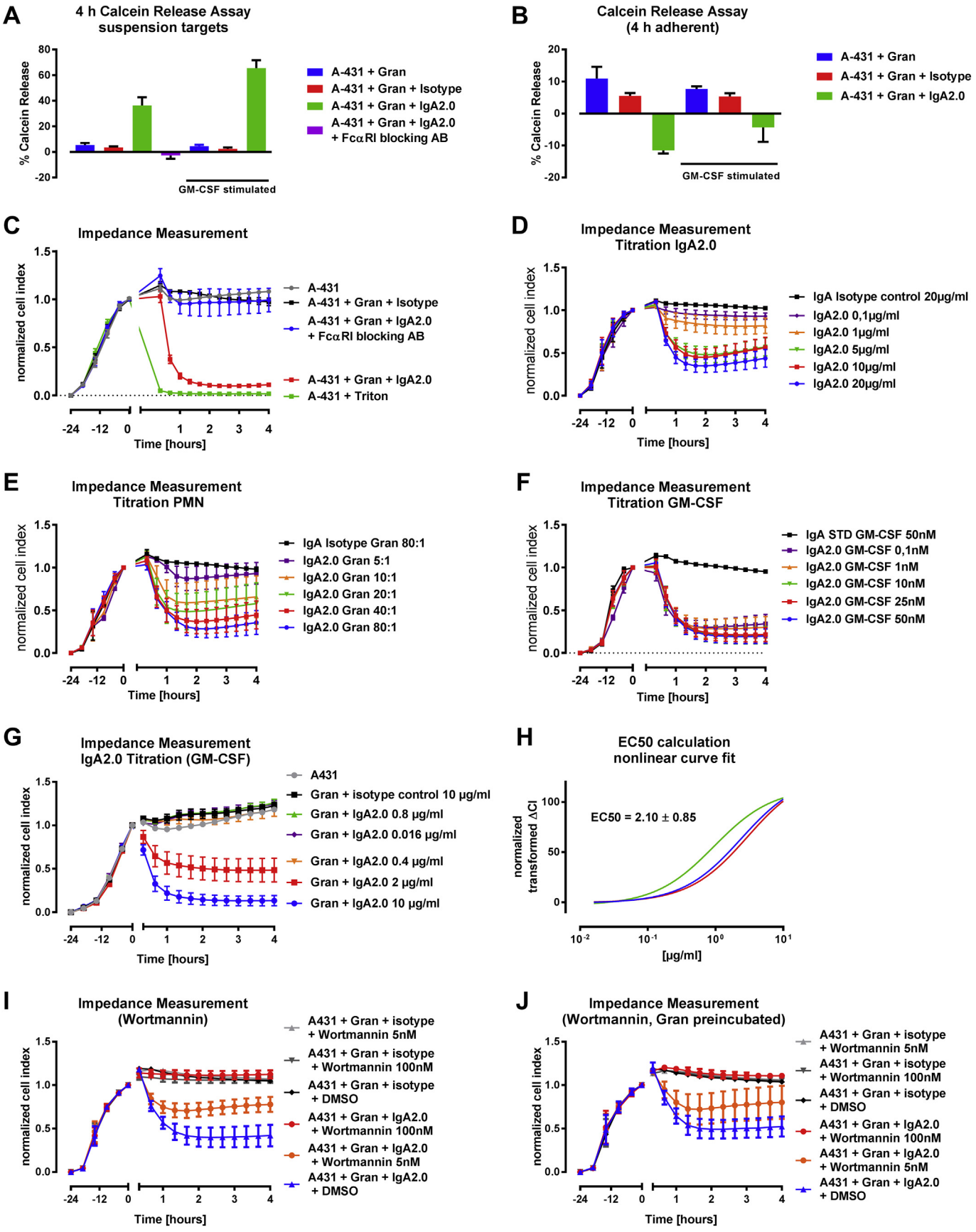

Fig. 1. Calcein release and impedance as read-out system for the FcαRI-mediated effector mechanism ADCC.

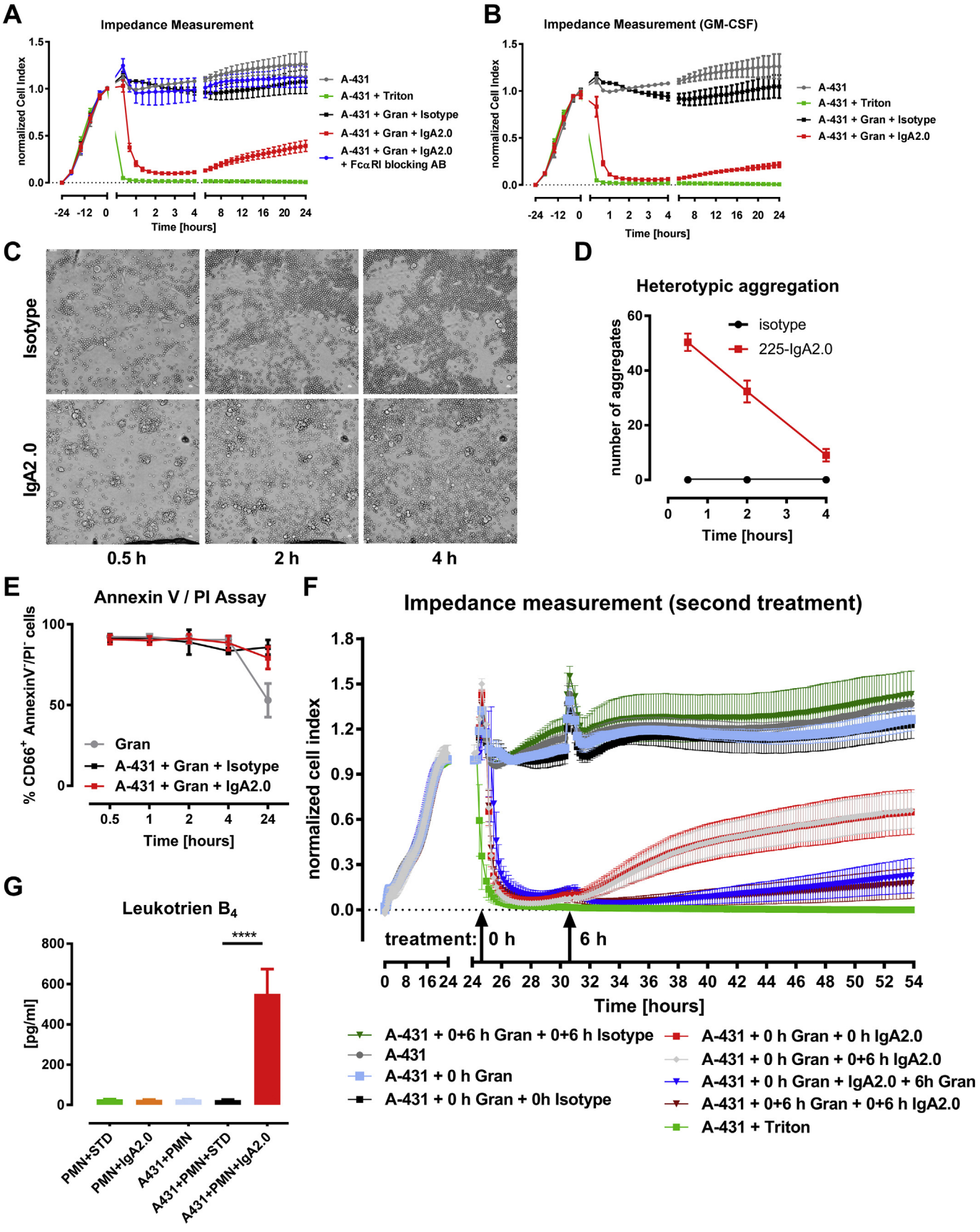

Fig. 2. Effector cell activity influences long-term efficacy.

granulocyte-mediated ADCC using adherently growing target cells. 2×10^4 A-431 target cells were seeded into the E-plates, grew to confluence for 24 h and were treated with 10 μg/ml 225-IgA2.0 and granulocytes (E:T ratio 40:1). The Cell-Index (CI) value, which reflects the impedance of the adherently growing target cells measured by the gold electrodes on the E-plate's bottom, was normalized to 1 (normalized CI (nCI)) at the time point of treatment. The CI value decreased rapidly within the first two hours reaching a maximum ΔCI compared to isotype control within 4 h (Δ CI 4 h = 0.84 ± 0.16, $n = 7$, $p < .0001$) if target cells were treated with granulocytes and 225-IgA2.0 (Fig. 1C). The effect was blocked completely by FcαRI inhibition using 10 μg/mL of the antibody A59 (91.2% adherent cells ± 17.1%) (Fig. 1C). This demonstrates the FcαRI-dependent activation of the granulocytes specifically by the EGFR-specific IgA antibody as measured previously using CRA and Calcein release assays (Lohse et al., 2016). The results further indicate a dependency of the ADCC on the concentration of the EGFR-specific 225-IgA2.0 (Fig. 1D). The minimal required concentration was 5 μg/ml and hence EC50 was significantly (3.36 ± 1.03 μg/ml, $p = .0034$) higher than using CRA with a previously reported EC50 of 0.75 ± 0.54 μg/ml (Lohse et al., 2016). The steady decline in impedance with lower antibody concentrations and granulocytes might be explained by a growth inhibiting low-level cytotoxicity. ADCC of adherent targets was enhanced with increasing E:T ratio (Fig. 1E) and GM-CSF stimulation (Fig. 1F), as previously shown for target cells in suspension using CRA (Lohse et al., 2016). We repeated the IgA2.0 titration using an E:T ratio (40:1) and GM-CSF concentration (25 nM) (Fig. 1G). Subsequent EC50 calculation (Fig. 1H) revealed an EC50 (2.10 ± 0.85 μg/ml IgA2.0) that is significantly higher ($p < .0001$) as previously published using CRA (EC50 = 0.14 ± 0.07 μg/ml) (Lohse et al., 2016). The results achieved with the impedance-based assay indicate that granulocyte-mediated ADCC of adherently growing target cells may require higher amounts of the specific antibody.

Next, we supplemented Wortmannin, an inhibitor of PI3K, a relevant kinase for FcαRI- signaling and neutrophil-mediated tumor cell killing via trogoptosis (Bakema et al., 2011; Matlung et al., 2018). Adding Wortmannin (Fig. 1I) or pre-incubation of the neutrophils (Fig. 1J) inhibited ADCC at 5 nM and prevented it at the 100 nM in both cases. Our results demonstrate that FcαRI-signaling is critical for neutrophil mediated killing of adherent target cells. Pre-treatment of target cells with Chloroquine (Suppl. Fig. 2), an inhibitor of autophagosome-lysosome fusion, had no effect. Thus, our results may suggest trogoptosis instead of autophagy as underlying killing mechanism (Bakema et al., 2011, Matlung et al., 2018). In summary at this point, the impedance-based assay allows the documentation of the FcαRI-dependent neutrophil-mediated killing proving previous observations using release assays but using adherently growing target cells.

Calcein release assay was conducted to investigate the capacity of the 225-IgA2.0 (10 μg/ml) to engage granulocytes for ADCC of A-431 targets cells in suspension (5×10^3, A) vs. adherence (2×10^4, B). (C) Impedance measurement was used as readout for the capacity of the 225-IgA2.0 (10 μg/ml) to engage granulocytes for ADCC of A-431 targets cells (2×10^4) with either unstimulated or GM-CSF (25 nM) stimulated granulocytes (E:T ratio 40:1). Effect of antibody concentration (D), E:T ratio (E), and GM-CSF stimulation (F) on the 225-IgA2.0- and granulocyte-dependent reduction of the impedance were measured. (G) Titration of the 225-IgA2.0 was performed using an E:T ratio of 40:1 and stimulation with 25 nm GM-CSF. (H) Normalized transformed ΔCI at 4 h end-point of each IgA2.0 concentration to isotype control of (G) were calculated and nonlinear curve fits of each single run for EC50 calculation are displayed. Effect of Wortmannin (I) and Wortmannin-pretreatment of the granulocytes (J) on the 225-IgA2.0- and granulocyte-dependent reduction of the impedance were measured. Data are presented as "% Calcein release" (A + B) or "normalized Cell Index" (C–G, I and J) as mean ± SEM of seven (A–C) or at least three (D–G, I and J) independent experiments run in triplicates. Gran = Granulocytes, IgA2.0 = 225-IgA2.0.

3.3. Long-term impedance monitoring allows the documentation of outgrowing target cells

Next, we investigated the long-time efficacy of the 225-IgA2.0-dependent granulocyte-mediated ADCC. Impedance monitoring for 24 h after treatment (conditions: 2×10^4 targets, 10 μg/ml of respective antibody, E:T ratio 40:1) revealed an increase in CI value starting 6 h irrespective of whether granulocytes were stimulated with GM-CSF (25 nM) or not (Fig. 2A and B). The increasing impedance after 6 h after treatment indicates reattachment and outgrowth of residual non-killed target cells, which was further delayed by GM-CSF primed granulocytes. Thus, despite a significant killing efficacy in the first 4 h, the possibility remains that residual non-killed target cells recover and grow out again.

3.4. Impedance-based long-term monitoring of effector cell activity

Then we investigated the impact of effector cell activity on the outgrowth of non-killed target cells. Live cell imaging of target and effector cells (Fig. 2C) revealed that at 30 min after treatment, granulocytes grouped at multiple numbers around target cells in the presence of the EGFR-specific 225-IgA2.0. During the following 4 h, we observed a substantial reduction of this heterotypic aggregation indicating a reduced granulocyte activity (Fig. 2C and D). No decrease in Annexin V and PI negative granulocytes was detected until 24 h after treatment indicating that effector cells were still alive but exhausted (Fig. 2E). The combined treatment of granulocytes with GM-CSF, which is released by A-431 cells and promotes their survival (Kapp et al., 1987, Colotta et al., 1992 Blood), and soluble IgA could be responsible for the higher number of Annexin V and PI negative granulocytes (Schettini et al., 2002, Wehrli et al., 2014).

To test the hypothesis of exhausted granulocytes we supplemented fresh (GM-CSF-primed, 25 μM) granulocytes at 6 h after treatment (Fig. 2F). At 54 h after treatment (24 h after the second treatment) we detected nCI values of 0.65 ± 0.26 and 0.18 ± 0.18 ($p = .0374$) for A-431 cells treated once and twice with IgA2.0 and granulocytes, respectively, demonstrating an improved ADCC activity. The nCI were 1.23 ± 0.16 and 1.43 ± 0.27 for single and double treatment with isotype control and granulocytes (compared to respective IgA2.0 treatment $p = .0043$ and $p \leq .0001$) proving the non-cytotoxic effect of granulocytes using an irrelevant antibody. Adding fresh granulocytes alone to cells treated once with granulocytes and isotype or IgA2.0 resulted in nCI at 54 h of 1.27 ± 0.03 and 0.23 ± 0.20, respectively ($p = .0001$). The results demonstrated that adding fresh granulocytes alone was sufficient to prolong the ADCC activity, whereas adding fresh antibody only was not (Fig. 2F). No significantly increased nCI for A-431 treated twice with granulocytes and IgA2.0 or once with fresh granulocytes added at 6 h compared to Triton X control was detected at 54 h, respectively.

Interestingly, previous studies reported the specific release of LTB_4, a potent attractant for neutrophils, upon IgA-dependent FcαRI-cross-linking on neutrophils (van der Steen et al., 2009). In line with this report, we could demonstrate the specific release of LTB_4 during the IgA2.0-dependent granulocyte-mediated ADCC (Fig. 2G). Thus, an LTB_4-dependent recruitment of fresh neutrophils could result in an ongoing ADCC activity.

Monitoring of IgA-dependent ADCC of A-431 was extended to 24 h using granulocytes without- (A) and with GM-CSF stimulation (B). FcαRI interaction was blocked by addition of 10 μg/ml anti-CD89 antibody A59 in (A). (C) Representative pictures from live cell imaging of ADCC using adherent A-431 cells of three independent experiments at the time points 0.5, 2 and 4 h after treatment are displayed. Heterotypic aggregates of A-431 target and effector cells of three independent experiments were counted (D). (E) Granulocytes were stained with a

CD66b-specific BV421-labeled antibody and Annexin-V-APC/PI by flow cytometry. (F) A-431 targets cells (2×10^4) grew to confluence for 24 h and were treated with GM-CSF primed granulocytes (E:T 40:1) and respective antibodies (10 µg/ml) at 0 h and at 6 h and impedance was measured for additional 24 h. (G) Supernatants after 1 h of ADCC were analyzed for LTB_4 release by ELISA ($n = 4$). Data are presented as mean ± SEM of "normalized Cell Index" in A, B and F and as "[pg/ml]" in G of three independent experiments run in triplicates. Data are shown as "number of aggregates" in D and as "%$CD66b^+$ $AnnexinV^-/PI^-$ cells" in E as mean ± SD of three independent experiments. Gran = Granulocytes, IgA2.0 = 225-IgA2.0. Significant differences are displayed with asteriks: $****p \leq .0001$.

3.5. Validation of the impedance assay on cell lines representing a relevant tumor entity

Next, we applied the impedance-based assay on a panel of EGFR-expressing HNSCC lines to investigate their sensitivity to the IgA-granulocyte-based treatment approach. EGFR and granulocyte levels are critical clinical parameters in HNSCC, thus we mainly used SCC cell lines derived from different respective anatomical sites: CAL-33 and SAS (tongue SCC), FaDu (hypopharynx SCC), HN (oral cavity SCC), HSC4 and SAT (aero-digestive tract SCC), UM-SCC1 (floor of the mouth SCC). A-431 (epidermoid SCC) and KYSE-30 (esophagus SCC), which were previously published as sensitive using CRA, served as controls (Lohse et al., 2016).

The cell lines were investigated for their EGFR surface expression by flow cytometry (Fig. 3A), which was previously indicated as a marker for ADCC efficacy in CRA (Derer et al., 2013). A-431 and Kyse30 cells displayed the highest EGFR surface level, followed by SAT, HSC-4, HN, FaDu, CAL-33, UM-SCC-1 with medium and SAS with the lowest surface expression. We then investigated the efficacy of IgA2.0-dependent granulocytes mediated ADCC using the impedance-based assay (conditions: 2 × 104 targets, 10 µg/ml of respective antibody, E:T ratio 40:1, GM-CSF: 25 nM). With the intention to simulate results of a respective release assay, we displayed the nCI of target cells treated with GM-CSF primed granulocytes and isotype control or 225-IgA2.0 at 4 h after treatment, respectively (Fig. 3B). We measured a significantly and specifically reduced impedance for all cell lines with the exception of SAS and HN. Notably, A-431, Kyse-30 and SAT, the target cells with the highest EGFR surface level, displayed the most significant reduction. In line with a previous report, the individual ΔCI (difference of bars in Fig. 3B) correlated with the EGFR surface level (Derer et al., 2013) (Fig. 3C).

EGFR surface expression was analyzed by flow cytometry and indirect immunofluorescence using a mouse anti-human EGFR antibody and the PE-labeled mIgGκ binding protein. Results were normalized to the mean value of all cell lines and are displayed as RFI of EGFR surface expression as mean ± SD of three independent experiments. (B) The individual nCI was calculated of target cells treated with GM-CSF primed granulocytes and isotype control and 225-IgA2.0 at 4 h after treatment, respectively. Results are presented as "nCI 4 h" as mean ± SEM of at least three independent experiments run in triplicates. Significant differences are displayed with asterisk: $*p \leq .05$, $**p \leq .01$, $***p \leq .001$, $****p \leq .0001$. (C) Correlation of ΔCI (difference of bars in B) with EGFR surface level (in A) at 4 h after treatment was calculated as Pearson correlation coefficient r. Significant correlations are displayed with asterisk: $*p \leq .05$.

3.6. Neither kinetics nor long-term efficacy of IgA-graulocyte-ADCC correlate with EGFR surface level

The kinetics within the first 4 h after treatment reflect the potency of the 225-IgA2.0 to activate granulocytes for an efficient ADCC of adherently growing target cells. In addition to the ΔCI at 4 h, the IC50 (time point of 50% reduction) and the area under curve (AUC) were calculated to describe the individual kinetics (Table 1). The fastest reduction of impedance was measured for the cell lines A-431 and KYSE-30 with the highest EGFR level (Fig. 4A and B), followed by the cell lines SAT, UM-SCC-1 and FaDu with a slightly slower reduction if

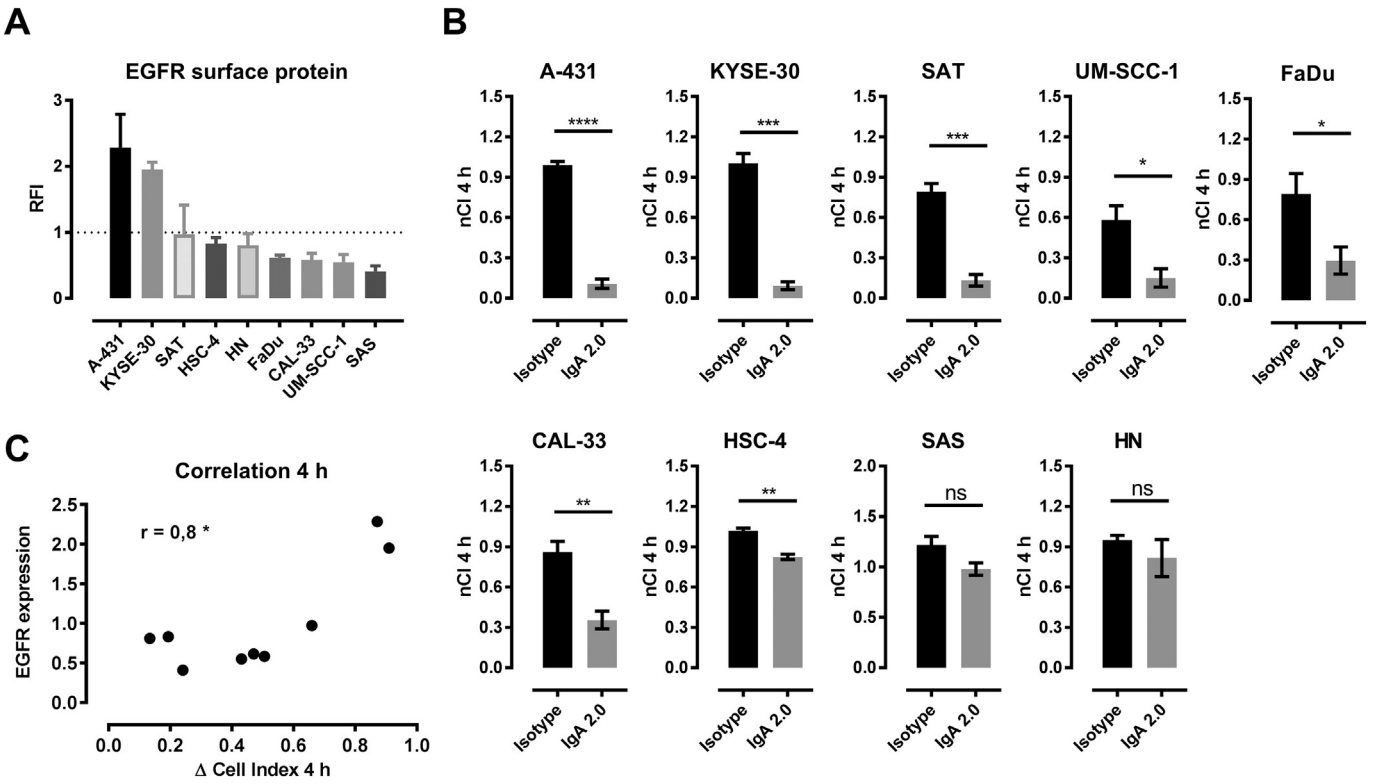

Fig. 3. The 4 h end-point result correlates with EGFR surface expression.

Table 1
Short-time kinetic parameters of granulocyte-mediated ADCC.

Cell line	IC50 [min]	AUC
A-431	44.4 ± 10.8	114.2 ± 29.5
KYSE-30	40.1 ± 5.9	105.7 ± 12.5
SAT	72.0 ± 14.4	157.9 ± 31.0
UM-SCC-1	47.1 ± 19.7	121.8 ± 35.7
FaDu	51.2 ± 8.4	124.6 ± 23.7
Cal33	89.7 ± 17.4	193.8 ± 41.4
HSC-4	42.2 ± 10.7	283.6 ± 34.3
SAS	66.0 ± 49.8	256.0 ± 14.2
HN	34.6 ± 6.1	243.2 ± 54.0

IC50 = time point at 50% reduced impedance, AUC = area under curve.

treated with 225-IgA2.0 and granulocytes (Fig. 4C–E). Respective treatment of the cell line CAL-33 displayed a slower reduction compared to A-431 for instance with a two-fold higher IC50 (Fig. 4F). In case of the cell lines SAS, HSC-4, and HN the weak ADCC effectivity mirrored a flat kinetic (Fig. 4G–I). There was a weak but not significant reciprocal correlation of the AUC with the EGFR surface expression ($r = -0.54$, $p = .0649$). The results indicate that the EGFR surface expression influences but it does not sufficiently predict the short-term ADCC kinetics.

The documentation of long-term kinetics (until 24 h after treatment) elucidates the long-lasting efficiency of the 225-IgA2.0-dependent granulocytes-mediated ADCC. It answers the question if the ADCC activity within the first 4 h was efficient enough to prevent the outgrowth of residual non-killed target cells. In case of A-431 and Kyse-30 cells treated with 225-IgA2.0 and granulocytes, after 8 h the impedance started to increase until 24 h of monitoring indicating outgrowth of non-killed target cells in both cases (Fig. 4A and B). A sustained reduction of the impedance was detected for the HNSCC lines SAT, UM-SCC-1 and FaDu if treated with 225-IgA2.0 and granulocytes (Fig. 4C–E). UM-SCC-1 and FaDu cells were sensitive to GM-CSF primed granulocytes alone mirrored by an antibody-independent steady decline in impedance (Fig. 4D and E). Despite the significantly reduced nCI at 4 h after treatment, CAL-33 cells completely recovered to confluence within 24 h (Fig. 4F). The minimal ADCC of HSC-4, SAS and HN cells within the first 4 h was not sufficient to prevent the complete recovery of all three cell lines (Fig. 4G–I). Based on the data we may conclude that high EGFR levels do not guarantee a complete treatment success. Moreover, the rather cell line specific results of the impedance-based assays point to additional factors critical for neutrophil-mediated ADCC.

(A–I) 2×10^4 cells of the indicated cell line were seeded per well in E-96 well plates 24 h prior to addition of respective antibody (10 µg/ml) and GM-CSF (25 nM) stimulated granulocytes (E:T ratio 40:1). Impedance was measured for 24 h before and after treatment using

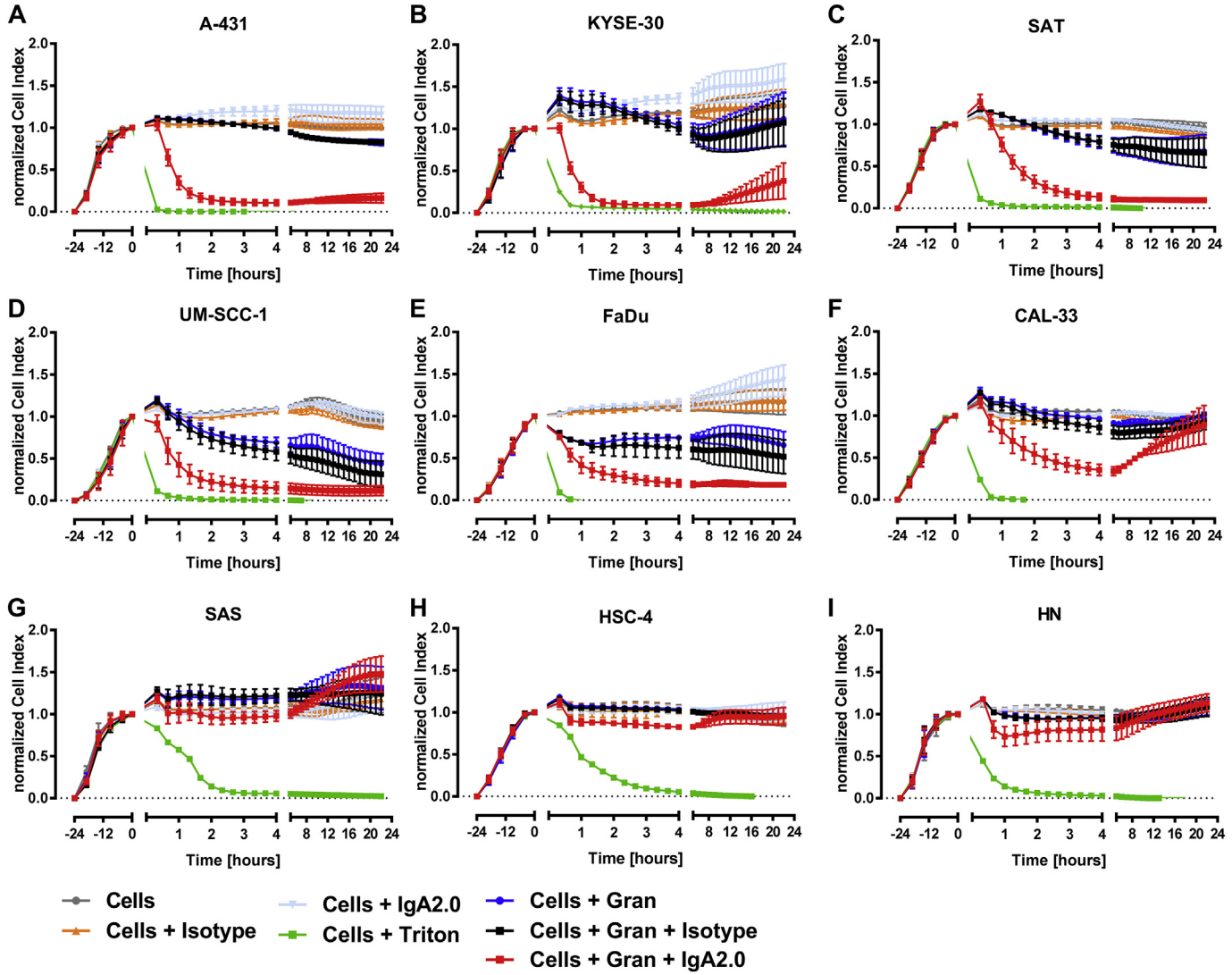

Fig. 4. Sensitivity of EGFR-expressing tumor cell lines to granulocytes and EGFR-specific 225-IgA2.0-mediated ADCC.

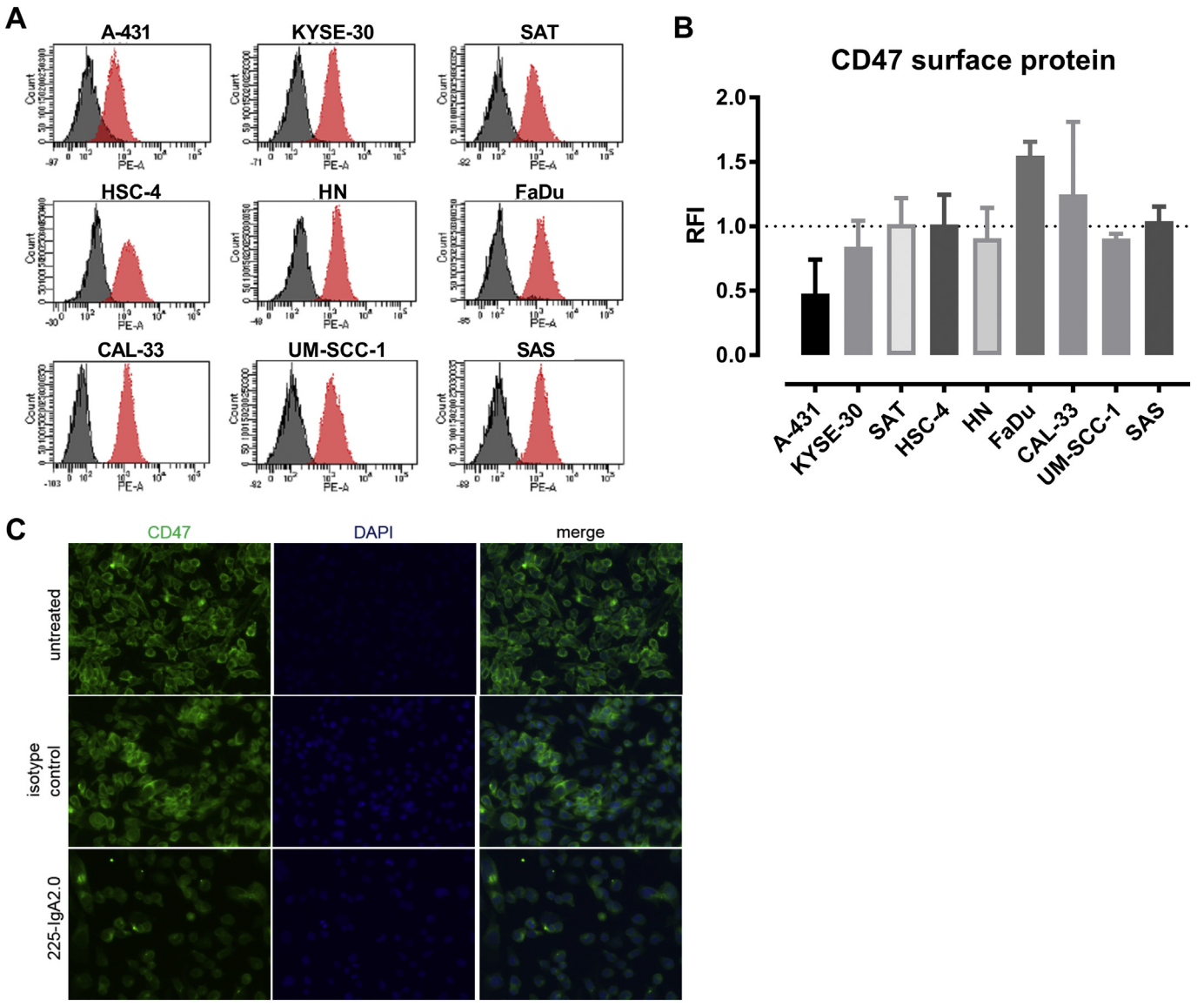

Fig. 5. CD47 surface level on target cells: (A) The surface expression of CD47 was analyzed by indirect immunofluorescence and flow cytometry using a human-CD47 specific antibody and the mIgG1-BP-PE. Representative histograms of three independent experiments are displayed. (B) Fluorescence intensity in relation to the isotype control and normalized to the mean of all cell lines is displayed as mean ± SD as "RFI" of three independent experiments. (C) A-431 target cells were harvested 72 h after treatment from the E-plates by trypsinization and seeded into black µ-clear flat bottom 96-well plates. Outgrowing target cells were stained by indirect immunofluorescence using a mouse-anti-human CD47 specific primary and an AlexaFluor-488-labeled anti-mouse secondary antibody. DAPI was used for nuclear co-staining. Representative pictures of three independent experiments are displayed.

15 min intervals. Data are presented as the mean ± SEM of "normalized Cell Index" of at least three independent experiments run in triplicates. Gran = Granulocytes, IgA2.0 = 225-IgA2.0.

3.7. CD47 surface expression is not predictive for ADCC efficacy

CD47 was reported as a limiting factor for trogoptosis, a mechanism of IgG-FcγR-dependent neutrophil-mediated tumor cell killing (Matlung et al., 2018). Consequently, blocking this axis enhanced IgG-dependent ADCC. Our preliminary results (Fig. 1, Suppl. Fig. 2) suggested IgA-FcαRI-dependent trogoptosis as a relevant mechanism. Subsequently, we investigated CD47 expression by flow cytometry (Fig. 5A and B). The highest CD47 surface level was detected on the cell line FaDu, the lowest on A-431 and similar high not significantly different levels on the residual cell lines. To investigate if CD47 effects long-term survival, A-431 cells harvested after 72 h ADCC from the E-plates, reseeded onto black 96-well plates were stained for CD47 expression by immunofluorescence 48 h afterwards. We observed an overall lower fluorescence intensity on surviving and outgrowing target cells treated with the EGFR-specific 225-IgA2.0 and granulocytes compared to isotype and untreated control (Fig. 5B) without any significant difference in morphology. We may conclude that CD47 is not a limiting factor for IgA-FcαRI-dependent neutrophil-mediated ADCC of adherent target cells.

3.8. Excess expression of Mac1 ligands limits long-term ADCC efficacy

Mac1 has been identified earlier as essential for the FcαRI-dependent engagement of granulocytes for ADCC (van Spriel et al., 2001). We questioned if the presence of Mac1 ligands, ICAM1 for instance, may facilitate IgA-neutrophil-ADCC and investigated the expression of ICAM1 by qRT-PCR (mRNA level, Fig. 6A) and by flow cytometry (surface protein level, Fig. 6B). Interestingly, the two cell lines, HN and HSC-4, with an apparently sufficient EGFR surface level but lacking

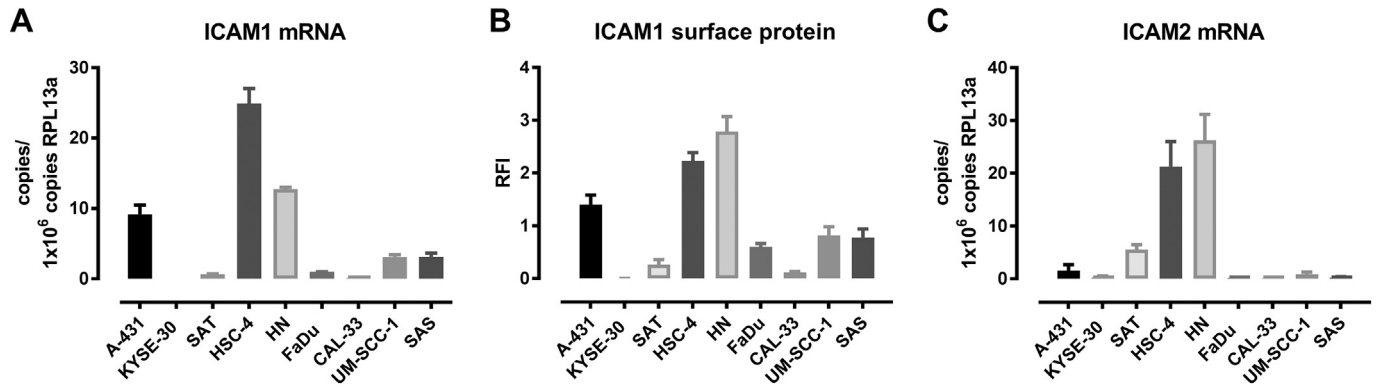

Fig. 6. Expression of the Mac1 ligands ICAM1 and ICAM2: (A) ICAM1 mRNA was quantified by qRT-PCR and normalized to the housekeeping gene RPL13a. (B) Expression of ICAM1 protein on the cell's surface was analyzed by flow cytometry and indirect immunofluorescence staining with a mouse anti-human ICAM1 antibody and the PE-labeled mIgG1-binding protein. The mean fluorescence intensity (MFI) was related to the respective isotype control. (C) ICAM2 mRNA was quantified by qRT-PCR and normalized to the housekeeping gene RPL13a. Data are presented as "mean ± SD" of "copies/1x10^6 copies RPL13a" in A and C, as "RFI" in B of three independent experiments. Results were normalized to the mean value of all cell lines.

sensitivity to IgA-neutrophil-ADCC, expressed the highest levels of ICAM1 mRNA and surface protein. We analyzed the mRNA expression of an additional Mac1 ligand, ICAM2 (Fig. 6C), and again HN and HSC-4 displayed the highest mRNA levels. On the other site, cell lines not expressing both or none of the two Mac1 ligands, were sensitive to the IgA-neutrophil-ADCC. Correlation analysis revealed a positive but not significant Pearson r coefficient for all three parameters to the long-term kinetic parameter AUC (Table 1): ICAM1 mRNA (r = 0.5845, p = .0984), ICAM1 surface protein level (r = 0.6384, p = .06384) and ICAM2 mRNA level (r = 0.6657, p = .0503). Our results suggest that excess expression of more than one Mac1 ligand might impair the IgA-neutrophil-ADCC in case of non-excess antigen levels on adherent targets cells.

4. Discussion

With this report, we demonstrated for the first time the kinetics of neutrophil-mediated ADCC using the label-free impedance-based technology. We monitored in real-time the efficacy of an engineered EGFR-directed IgA2-antibody to engage granulocytes for the ADCC of adherently growing EGFR-expressing target cells. The electrical impedance was reduced upon ADCC-related detachment or membrane disintegration (Glamann and Hansen, 2006; Peper et al., 2014; Seidel et al., 2014; Tóth et al., 2017) specifically upon the treatment with the EGFR-directed 225-IgA2.0 and granulocytes. Blocking the binding to and the downstream signaling of the FcαRI abrogated neutrophil-mediated ADCC and suggested a trogoptosis-like mechanism of the IgA-neutrophil-ADCC (Matlung et al., 2018). Thus, the impedance-based approach provided comparable results to previously used ^{51}chromium and Calcein release assays (Lohse et al., 2016) but in contrast to these permits investigations on adherently growing cancer target cells.

The anchorage-dependent growth of target cells alters the expression and distribution of lipid rafts containing EGFR (Gao et al., 2015), while anchorage-independent EGFR signaling seems to facilitate the sensitivity to EGFR targeting antibodies (Ohnishi et al., 2015; Braunholz et al., 2016). This may modify the requirements for a successful synapse formation, for instance significantly higher amounts of antibody. Indeed, mean serum levels of 0.1 to 0.15 µg/ml were sufficient in a xenogeneic animal model using A-431 target cells and FcαRI-transgenic mice (Lohse et al., 2016). However, there is lacking information if target cells in vivo grew indeed adherently in the peritoneum or in an anchorage-independent manner and on clinical data on IgA antibodies in humans. Based on our results, this model may not accurately reflect the physiologic situation in humans with tissue residing adherently growing tumor cells.

CD47 limits IgG-FcγR-dependent neutrophil ADCC via trogoptosis in the context of inhibitory FcγR-signaling and target cells in suspension using CRA (Matlung et al., 2018). Although our results at the beginning indicate a similar killing mechanism, CD47 seems to be dispensable for the IgA-FcαRI-dependent neutrophil-ADCC in the anchorage-dependent context lacking inhibitory Fc receptor signaling. Moreover, PI3K was described as central player in cytokine mediated inside-out signaling (Bakema et al., 2011), which may explain the observed sensitivity of the IgA-neutrophil-ADCC to Wortmannin as well.

Mac1 is essential in the FcαRI-dependent immunologic synapse formation (van Spriel et al., 2001; van Egmond et al., 1999). Expression of Mac1 ligands on target cells seems to facilitate IgG-FcγR-dependent neutrophil and NK-cell ADCC (Textor et al., 2011, Matlung et al., 2018). However, excess surface levels of more than one ligand may disturb synapse formation in the anchorage-dependent context with limited EGFR surface level and membrane flexibility reducing cross-linking abilities of EGFR-targeting antibodies. This could result in the observed insensitivity of the two cell lines HN and HSC-4, while ICAM-negative cells (KYSE-30) or ICAM1-expressing cells (A-431), both with excess antigen surface level, are efficiently killed by the IgA-neutrophil ADCC (also using CRA, Lohse et al., 2016). Our results suggest a critical role of Mac1 ligands for the IgA-FcαRI-dependent neutrophil-ADCC of adherent target cells depending on the antigen level.

The ADCC efficacy correlated with the EGFR expression at 4 h after treatment, which is in line with previous data obtained with CRA (Derer et al., 2013). Five of seven HNSCC lines displayed a significant sensitivity to the treatment, with a continuous decline of impedance within 24 h recorded for three of these. EGFR overexpression is frequent in HNSCC and high levels of EGFR as well as neutrophil counts at the invasive front mark patients at higher risk for poor prognosis (Spano et al., 2005; Rao et al., 2012; Dumitru et al., 2013; Meriggi et al., 2017). Thus, our findings support the IgA-FcαRI-neutrophil approach as a promising alternative immunotherapeutic concept for this subgroup of HNSCC patients.

Direct tumor cell killing by neutrophils has been reported and reviewed earlier (Fridlender and Albelda, 2012). In our case it might be related to the combined effect of critical antigen and Mac1 ligand levels, expression of Fas ligand, by which tumor cells may escape the attack (Chen et al., 2003), and the release of activating chemokines (data not shown). These may lead to a partial degranulation and release of toxic components in the absence of specific IgA antibodies and explain the susceptibility of tumor cells to anti-tumorigenic neutrophils.

The IgA-granulocyte-ADCC resulted in the specific release of LTB_4, a potent attractant of neutrophils that in turn will recruit new effector cells (van der Steen et al., 2009). Providing fresh neutrophils rescued

ADCC activity and might be required for a sustained treatment response of individual target cells since neutrophils seem to exhaust within 4 h of treatment. Our data support the previously indicated hypothesis of an IgA-neutrophil-dependent self-fueling tumor cell-killing loop (Heineke and van Egmond, 2016). This feed-forward loop could be potentiated in the background of human papillomavirus (HPV)-induced carcinogenesis with active myeloid cell recruitment (Schröer et al., 2011). In HNSCC, HPV displays a relevant prognostic variable influencing the expression of EGFR, CD47, ICAM1 and therapy outcome (Reimers et al., 2007; Mirghani et al., 2014; Liu et al., 2018). Further investigations are required to determine the immunotherapeutic potential of the IgA-FcαRI-neutrophil approach targeting HPV-positive HNSCC, since HPV oncoproteins modulate all of the above-investigated parameters.

5. Conclusions

The impedance-based assay allows the real-time monitoring of IgA-dependent granulocyte-mediated ADCC using adherently growing solid cancer target cells. It provided valuable information on the kinetics and effector cell activity during IgA-FcαRI-granulocyte dependent ADCC. Effector cell exhaustion together with critical expression levels of EGFR and Mac1 ligands might display important factors to predict long-term efficacy and target cell resistance, while the don't eat me signal CD47 seems dispensable. Thus, the impedance-based ADCC assay displays a promising tool to identify additional critical parameters for IgA-FcαRI-dependent neutrophil-mediated ADCC.

Acknowledgments

We gratefully acknowledge the excellent technical assistance from Jessica Schmitt-Bennewart, Katrin Thieser and Barbara Best, for Dr. Malte Kriegs and Prof. Dr. Mascha Binder (University Medical Center Hamburg-Eppendorf, Oncology Center, Department for Radiotherapy and Radio-Oncology) and for Florian Bochen (Department of Otorhinolaryngology, Head and Neck Surgery; Saarland University Medical Center, Homburg/Saar, Germany) for kindly providing the HNSCC lines, Prof. Dr. Thomas Valerius (University Hospital Schleswig-Holstein, Division of Stem Cell Transplantation and Immunotherapy, II. Department of Internal Medicine) for the great help with the 225-IgA2.0 antibody and Prof. Dr. Kerstin Junker (Department of Urology, Saarland University Medical Center, 66421, Homburg/Saar, Germany) and Prof. Dr. Richard Zimmermann (Institute of Medical Biochemistry & Molecular Biology, Saarland University, 66421 Homburg, Germany) for the great help with the xCELLigence units.

Funding

The German Research Organization (DFG, Lo1853/1-2) and intramural funding (HOMFOR) supported this work.

Appendix A. Supplementary data

Supplementary data to this article can be found online at https://doi.org/10.1016/j.jim.2019.112644.

References

Bakema, J.E., Ganzevles, S.H., Fluitsma, D.M., Schilham, M.W., Beelen, R.H., Valerius, T., Lohse, S., Glennie, M.J., Medema, J.P., van Egmond, M., 2011 Jul 15. Targeting FcαRI on polymorphonuclear cells induces tumor cell killing through autophagy. J. Immunol. 187 (2), 726–732. https://doi.org/10.4049/jimmunol.1002581.

Boross, P., Lohse, S., Nederend, M., Jansen, J.H.M., van Tetering, G., Dechant, M., Peipp, M., Royle, L., Liew, L.P., Boon, L., et al., 2013. IgA EGFR antibodies mediate tumour killing in vivo. EMBO Mol. Med. 5 (8), 1213–1226. https://doi.org/10.1002/emmm.201201929.

Brandsma, A.M., ten Broeke, T., Nederend, M., Meulenbroek, L.A.P.M., van Tetering, G., Meyer, S., Jansen, J.H.M., Buitrago, M.A.B., Nagelkerke, S.Q., Németh, I., et al., 2015. Simultaneous targeting of FcγRs and FcαRI enhances tumor cell killing. Cancer Immunol. Res. 3 (12), 1316–1324. https://doi.org/10.1158/2326-6066.CIR-15-0099-T.

Braster, R., O'Toole, T., van Egmond, M., 2014. Myeloid cells as effector cells for monoclonal antibody therapy of cancer. Methods 65 (1), 28–37. https://doi.org/10.1016/j.ymeth.2013.06.020.

Braunholz, D., Saki, M., Niehr, F., Öztürk, M., Borràs Puértolas, B., Konschak, R., Budach, V., Tinhofer, I., 2016. Spheroid culture of head and neck cancer cells reveals an important role of EGFR signalling in anchorage independent survival. PLoS One 11 (9), e0163149. https://doi.org/10.1371/journal.pone.0163149.

Brunner, K.T., Mauel, J., Cerottini, J.-C., Chapuis, B., 1968. Quantitative assay of the lytic action of immune lymphoid cells of 51Cr-labelled allogeneic target cells in vitro; inhibition by isoantibody and by drugs. Immunology 14 (2), 181–196.

Chen, Y.L., Chen, S.H., Wang, J.Y., Yang, B.C., 2003 Aug 1. Fas ligand on tumor cells mediates inactivation of neutrophils. J. Immunol. 171 (3), 1183–1191.

Colotta, F., Re, F., Polentarutti, N., Sozzani, S., Mantovani, A., 1992 Oct 15. Modulation of granulocyte survival and programmed cell death by cytokines and bacterial products. Blood 80 (8), 2012–2020.

Derer, S., Lohse, S., Valerius, T., 2013. EGFR expression levels affect the mode of action of EGFR-targeting monoclonal antibodies. Oncoimmunology 2 (5), e24052. https://doi.org/10.4161/onci.24052.

Dumitru, C.A., Lang, S., Brandau, S., 2013. Modulation of neutrophil granulocytes in the tumor microenvironment: mechanisms and consequences for tumor progression. Semin. Cancer Biol. 23 (3), 141–148. https://doi.org/10.1016/j.semcancer.2013.02.005.

Fridlender, Z.G., Albelda, S.M., 2012 May. Tumor-associated neutrophils: friend or foe? Carcinogenesis 33 (5), 949–955. https://doi.org/10.1093/carcin/bgs123.

Galdiero, M.R., Garlanda, C., Jaillon, S., Marone, G., Mantovani, A., 2013. Tumor associated macrophages and neutrophils in tumor progression. J. Cell. Physiol. 228 (7), 1404–1412. https://doi.org/10.1002/jcp.24260.

Gao, J., Wang, Y., Cai, M., Pan, Y., Xu, H., Jiang, J., Ji, H., Wang, H., 2015. Mechanistic insights into EGFR membrane clustering revealed by super-resolution imaging. Nanoscale 7 (6), 2511–2519. https://doi.org/10.1039/c4nr04962d.

Glamann, J., Hansen, A.J., 2006. Dynamic detection of natural killer cell-mediated cytotoxicity and cell adhesion by electrical impedance measurements. ASSAY Drug Dev. Technol. 4 (5), 555–563. https://doi.org/10.1089/adt.2006.4.555.

Grandis, J.R.J.R., Tweardy, D.J.D.J., 1993. Elevated Llevels of Ttransforming Ggrowth Ffactor α and Eepidermal Ggrowth Ffactor Rreceptor Mmessenger RNA Aare Eearly Mmarkers of Ccarcinogenesis in Hhead and Nneck cancer. Cancer Res. 53 (15), 3579–3584.

Hanahan, D., Weinberg, R.A., 2011. Hallmarks of cancer: the next generation. Cell 144 (5), 646–674. https://doi.org/10.1016/j.cell.2011.02.013.

Heemskerk, N., van Egmond, M., 2018. Monoclonal antibody-mediated killing of tumour cells by neutrophils. Eur. J. Clin. Investig. (48 Suppl 2), e12962. https://doi.org/10.1111/eci.12962.

Heineke, M.H., van Egmond, M., 2016. Immunoglobulin A: magic bullet or Trojan horse? Eur. J. Clin. Investig. 47 (2), 184–192. https://doi.org/10.1111/eci.12716.

Hynes, N.E., MacDonald, G., 2009. ErbB receptors and signaling pathways in cancer. Curr. Opin. Cell Biol. 21 (2), 177–184. https://doi.org/10.1016/j.ceb.2008.12.010.

Kapp, A., Danner, M., Luger, T.A., Hauser, C., Schöpf, E., 1987. Granulocyte-activating mediators (GRAM). II. Generation by human epidermal cells—relation to GM-CSF. Arch. Dermatol. Res. 279 (7), 470–477.

Kute, T., John, R., Stehle, J., Ornelles, D., Walker, N., Delbono, O., Vaughn, J.P., 2012. Understanding key assay parameters that affect measurements of trastuzumab-mediated ADCC against Her2 positive breast cancer cells. Oncoimmunology 1 (6), 810–821. https://doi.org/10.4161/onci.20447.

Leemans, C.R., Braakhuis, B.J.M., Brakenhoff, R.H., 2011. The molecular biology of head and neck cancer. Nat. Rev. Cancer 11 (1), 9–22. https://doi.org/10.1038/nrc2982.

Liu, F., Dai, M., Xu, Q., Zhu, X., Zhou, Y., Jiang, S., Wang, Y., Ai, Z., Ma, L., Zhang, Y., et al., 2018. SRSF10-mediated IL1RAP alternative splicing regulates cervical cancer oncogenesis via mIL1RAP-NF-κB-CD47 axis. Oncogene 37 (18), 2394–2409. https://doi.org/10.1038/s41388-017-0119-6.

Lohse, S., Meyer, S., Meulenbroek, L.A.P.M., Jansen, J.H.M., Nederend, M., Kretschmer, A., Klausz, K., Möginger, U., Derer, S., Rösner, T., et al., 2016. An anti-EGFR IgA that displays improved pharmacokinetics and myeloid effector cell engagement in vivo. Cancer Res. 76 (2), 403–417. https://doi.org/10.1158/0008-5472.CAN-15-1232.

Lohse, S., Loew, S., Kretschmer, A., Marco, Jansen J.H., Meyer, S., ten Broeke, T., Rösner, T., Dechant, M., Derer, S., Klausz, K., et al., 2018. Effector mechanisms of IgA antibodies against CD20 include recruitment of myeloid cells for antibody-dependent cell-mediated cytotoxicity and complement-dependent cytotoxicity. Br. J. Haematol. 181 (3), 413–417. https://doi.org/10.1111/bjh.14624.

Marthaler, A.M., Podgorska, M., Feld, P., Fingerle, A., Knerr-Rupp, K., Grässer, F., Smola, H., Roemer, K., Ebert, E., Kim, Y.-J., et al., 2017. Identification of C/EBPα as a novel target of the HPV8 E6 protein regulating miR-203 in human keratinocytes. PLoS Pathog. 13 (6), e1006406. https://doi.org/10.1371/journal.ppat.1006406.

Matlung, H.L., Babes, L., Zhao, X.W., van Houdt, M., Treffers, L.W., van Rees, D.J., Franke, K., Schornagel, K., Verkuijlen, P., Janssen, H., et al., 2018 Jun 26. Neutrophils kill antibody-opsonized cancer cells by trogoptosis. Cell Rep. 23 (13). https://doi.org/10.1016/j.celrep.2018.05.082. 3946-3959.e6.

Meriggi, F., Codignola, C., Beretta, G.D., Ceresoli, G.L., Caprioli, A., Scartozzi, M., Fraccon, A.P., Prochilo, T., Ogliosi, C., Zaniboni, A., 2017. Significance of neutrophil-to-lymphocyte ratio in Western advanced EGFR-mutated non-small cell lung cancer receiving a targeted therapy. Tumori. 103 (5), 443–448. https://doi.org/10.5301/tj.5000632.

Mirghani, H., Amen, F., Moreau, F., Guigay, J., Hartl, D.M., Lacau, S.T., Guily, J., 2014. Oropharyngeal cancers: relationship between epidermal growth factor receptor alterations and human papillomavirus status. Eur. J. Cancer 50 (6), 1100–1111.

https://doi.org/10.1016/j.ejca.2013.12.018.
Oberg, H.-H., Peipp, M., Kellner, C., Sebens, S., Krause, S., Petrick, D., Adam-Klages, S., Röcken, C., Becker, T., Vogel, I., et al., 2014. Novel bispecific antibodies increase γδ T-cell cytotoxicity against pancreatic cancer cells. Cancer Res. 74 (5), 1349–1360. https://doi.org/10.1158/0008-5472.CAN-13-0675.
Ohnishi, Y., Yasui, H., Kakudo, K., Nozaki, M., 2015. Cetuximab-resistant oral squamous cell carcinoma cells become sensitive in anchorage-independent culture conditions through the activation of the EGFR/AKT pathway. Int. J. Oncol. 47 (6), 2165–2172. https://doi.org/10.3892/ijo.2015.3215.
Peper, J.K., Schuster, H., Löffler, M.W., Schmid-Horch, B., Rammensee, H.-G., Stevanović, S., 2014. An impedance-based cytotoxicity assay for real-time and label-free assessment of T-cell-mediated killing of adherent cells. J. Immunol. Methods 405, 192–198. https://doi.org/10.1016/j.jim.2014.01.012.
Rao, H.-L., Chen, J.-W., Li, M., Xiao, Y.-B., Fu, J., Zeng, Y.-X., Cai, M.-Y., Xie, D., 2012. Increased intratumoral neutrophil in colorectal carcinomas correlates closely with malignant phenotype and predicts patients' adverse prognosis. PLoS One 7 (1), e30806. https://doi.org/10.1371/journal.pone.0030806.
Reimers, N., Kasper, H.U., Weissenborn, S.J., Stützer, H., Preuss, S.F., Hoffmann, T.K., Speel, E.J., Dienes, H.P., Pfister, H.J., Guntinas-Lichius, O., et al., 2007. Combined analysis of HPV-DNA, p16 and EGFR expression to predict prognosis in oropharyngeal cancer. Int. J. Cancer 120 (8), 1731–1738. https://doi.org/10.1002/ijc.22355.
Roden, M.M., Lee, K.H., Panelli, M.C., Marincola, F.M., 1999. A novel cytolysis assay using fluorescent labeling and quantitative fluorescent scanning technology. J. Immunol. Methods 266 (1–2), 29–41.
Schettini, J., Salamone, G., Trevani, A., Raiden, S., Gamberale, R., Vermeulen, M., Giordano, M., Geffner, J.R., 2002 Oct. Stimulation of neutrophil apoptosis by immobilized IgA. J. Leukoc. Biol. 72 (4), 685–691.
Schröer, N., Pahne, J., Walch, B., Wickenhauser, C., Smola, S., 2011. Molecular pathobiology of human cervical high-grade lesions: paracrine STAT3 activation in tumor-instructed myeloid cells drives local MMP-9 expression. Cancer Res. 71 (1), 87–97. https://doi.org/10.1158/0008-5472.CAN-10-2193.
Seidel, U.J.E., Vogt, F., Grosse-Hovest, L., Jung, G., Handgretinger, R., Lang, P., 2014. γδ T cell-mediated antibody-dependent cellular cytotoxicity with CD19 antibodies assessed by an impedance-based label-free real-time cytotoxicity assay. Front. Immunol. 5, 618. https://doi.org/10.3389/fimmu.2014.00618.
Smola, S., 2017. Immunopathogenesis of HPV-associated cancers and prospects for immunotherapy. Viruses. 9 (9), 254. https://doi.org/10.3390/v9090254.
Spano, J.-P., Lagorce, C., Atlan, D., Milano, G., Domont, J., Benamouzig, R., Attar, A., Benichou, J., Martin, A., Morere, J.-F., et al., 2005. Impact of EGFR expression on colorectal cancer patient prognosis and survival. Ann. Oncol. 16 (1), 102–108. https://doi.org/10.1093/annonc/mdi006.
Szabó, B., Nelhűbel, G.A., Kárpáti, A., Kenessey, I., Jóri, B., Székely, C., Peták, I., Lotz, G., Hegedűs, Z., Hegedűs, B., et al., 2011. Clinical significance of genetic alterations and expression of epidermal growth factor receptor (EGFR) in head and neck squamous cell carcinomas. Oral Oncol. 47 (6), 487–496. https://doi.org/10.1016/j.oraloncology.2011.03.020.
Textor, S., Accardi, R., Havlova, T., Hussain, I., Sylla, B.S., Gissmann, L., Cerwenka, A., 2011 Mar 1. NF-κ B-dependent upregulation of ICAM-1 by HPV16-E6/E7 facilitates NK cell/target cell interaction. Int. J. Cancer 128 (5), 1104–1113. https://doi.org/10.1002/ijc.25442.
Tóth, G., Szöllősi, J., Vereb, G., 2017. Quantitating ADCC against adherent cells: impedance-based detection is superior to release, membrane permeability, or caspase activation assays in resolving antibody dose response. Cytometry Part A 91 (10), 1021–1029. https://doi.org/10.1002/cyto.a.23247.
Treffers, L.W., Hiemstra, I.H., Kuijpers, T.W., van den Berg, T.K., Matlung, H.L., 2016. Neutrophils in cancer. Immunol. Rev. 273 (1), 312–328. https://doi.org/10.1111/imr.12444.
Trellakis, S., Bruderek, K., Dumitru, C.A., Gholaman, H., Gu, X., Bankfalvi, A., Scherag, A., Hütte, J., Dominas, N., Lehnerdt, G.F., et al., 2011. Polymorphonuclear granulocytes in human head and neck cancer: enhanced inflammatory activity, modulation by cancer cells and expansion in advanced disease. Int. J. Cancer 129 (9), 2183–2193. https://doi.org/10.1002/ijc.25892.
Uribe-Querol, E., Rosales, C., 2015. Neutrophils in cancer: two sides of the same coin. J Immunol Res 983698. https://doi.org/10.1155/2015/983698.
Valero, C., Pardo, L., López, M., García, J., Camacho, M., Quer, M., León, X., 2016. Pretreatment count of peripheral neutrophils, monocytes, and lymphocytes as independent prognostic factor in patients with head and neck cancer. Head Neck 39 (2), 219–226. https://doi.org/10.1002/hed.24561.
van der Steen, L., Tuk, C.W., Bakema, J.E., Kooij, G., Reijerkerk, A., Vidarsson, G., Bouma, G., Kraal, G., de Vries, H.E., Beelen, R.H.J., et al., 2009. Immunoglobulin A: Fc(alpha) RI interactions induce neutrophil migration through release of leukotriene B4. Gastroenterology 137 (6). https://doi.org/10.1053/j.gastro.2009.06.047. 2018-2029.e1–3.
van Egmond, M., van Vuuren, A.J., Morton, H.C., van Spriel, A.B., Shen, L., Hofhuis, F.M., Saito, T., Mayadas, T.N., Verbeek, J.S., van de Winkel, J.G., 1999 Jun 15. Human immunoglobulin A receptor (FcalphaRI, CD89) function in transgenic mice requires both FcR gamma chain and CR3 (CD11b/CD18). Blood 93 (12), 4387–4394.
van Spriel, A.B., Leusen, J.H., van Egmond, M., Dijkman, H.B., Assmann, K.J., Mayadas, T.N., van de Winkel, J.G., 2001 Apr 15. Mac-1 (CD11b/CD18) is essential for Fc receptor-mediated neutrophil cytotoxicity and immunologic synapse formation. Blood. 97 (8), 2478–2486.
Wehrli, M., Cortinas-Elizondo, F., Hlushchuk, R., Daudel, F., Villiger, P.M., Miescher, S., Zuercher, A.W., Djonov, V., Simon, H.U., von Gunten, S., 2014 Dec 1. Human IgA Fc receptor FcαRI (CD89) triggers different forms of neutrophil death depending on the inflammatory microenvironment. J Immunol. 193 (11), 5649–5659. https://doi.org/10.4049/jimmunol.1400028.
Wierda, W.G., Mehr, D.S., Kim, Y.B., 1989. Comparison of fluorochrome-labeled and 51Cr-labeled targets for natural killer cytotoxicity assay. J. Immunol. Methods 122 (1), 15–24.
Woof, J.M., Russell, M.W., 2011. Structure and function relationships in IgA. Mucosal Immunol. 4 (6), 590–597. https://doi.org/10.1038/mi.2011.39.
Yamashita, M., Kitano, S., Aikawa, H., Kuchiba, A., Hayashi, M., Yamamoto, N., Tamura, K., Hamada, A., 2016 Jan 27. A novel method for evaluating antibody-dependent cell-mediated cytotoxicity by flow cytometry using cryopreserved human peripheral blood mononuclear cells. Sci. Rep. 6, 19772. https://doi.org/10.1038/srep19772.
Yamashita-Kashima, Y., Iijima, S., Yorozu, K., Furugaki, K., Kurasawa, M., Ohta, M., Fujimoto-Ouchi, K., 2011. Pertuzumab in combination with trastuzumab shows significantly enhanced antitumor activity in HER2-positive human gastric cancer xenograft models. Clin. Cancer Res. 17 (15), 5060–5070. https://doi.org/10.1158/1078-0432.CCR-10-2927.